INVESTIGATION OF ELECTRICAL AND MECHANICAL PROPERTIES OF TETRAGONAL/CUBIC COMPOSITE ELECTROLYTES PREPARED BY IMPREGNATION OF CUBIC ZIRCONIA WITH ZIRCONIA SOLUTION

M. Ghatee[1,*] and M.H. Shariat[2]

* *ghatee@yahoo.com*

Received: April 2010 **Accepted: January 2011**

[1] Faculty of Mechanical Engineering, Shahrood University of Technology, Shahrood, Iran.

[2] Department of Materials Science and Engineering, Shiraz University, Shiraz, Iran.

Abstract: *Zirconia solid electrolytes with nonequilibrium composite structure were prepared by impregnation of a porous 8YSZ matrix with a solution of Zirconia. Microstructures were characterized by XRD and SEM. The electrical properties were studied by impedance spectroscopy as a function of temperature. Biaxial flexural strength and fracture toughness of composite samples were measured by ring on ring and Vickers microhardness indentation methods respectively. The microstructures of the composite electrolytes were composed of cubic grains surrounded by tetragonal second phase grains. It was shown that the electrical and mechanical properties of the prepared electrolyte can be adjusted by controlling the amount of doped zirconia. Increasing the amount of doped zirconia increases the tetragonal phase content which improves fracture toughness and fracture strength. In addition, increasing tetragonal phase content of the composite electrolytes decreases the conductivity at high temperatures while the situation is reversed at low temperatures.*

Keywords: *Zirconia, Fuel Cell, Composite Electrolyte*

1. INTRODUCTION

8 mol% yttria stabilized zirconia 8YSZ shows the highest conductivity among the yttria doped zirconia solid electrolytes [1]. However, their low mechanical strength hinders the fabrication of self supported electrolyte with lower thickness or using for applications like oxygen sensors [2,3]. It has been reported that addition of second phase like Alumina [4], neodymium titanate [5], $BaTiO_3$ [6] or monoclinic zirconia [7] improve mechanical strength of 8YSZ but at the same time can degrade electrical properties [6].

3 mol% yttria stabilized zirconia with high mechanical strength ~ 1 GPa, high fracture toughness ~ 10 MPa $m^{1/2}$ and reasonable conductivity at 1000 °C is usually used to increase the mechanical properties of engineering ceramics [8]. It is well known that the presence of the tetragonal phase in partially stabilized zirconia PSZ based solid electrolytes improves mechanical properties. In PSZ electrolytes, the yttria content is adjusted at about 4- 6 mol% yttria which results in lower conductivity with respect to 8YSZ [9]. Composite materials can improve the combination of electrical and mechanical properties of materials to get the performance required for different applications. Various processing techniques have been reported for preparation of materials with composite structure. Among various processing techniques, net shape forming has a potential of preparing materials with core/shell structure. Net shape technology is combining powder processing and polymer precursor fabrication methods [10]. In this process powders form a framework of connected particles or net shape body, into which the polymeric precursor impregnates [10]. Upon heating at high temperatures, the polymer can decompose and a thin layer of related oxides is formed which fills the space between channels. After sintering at appropriate temperature, a dense body can be obtained [10]. This process has been used in many field of area of fuel cell and related topics [11, 12].

The aim of the present study is to prepare the 8YSZ/3YSZ composites with tetragonal zirconia core grains and yttria rich inter grain regions, perhaps with a core/shell microstructure via net shape forming. Fig. 1 summarizes the schematic steps of preparation of electrolytes with this structure by this method.

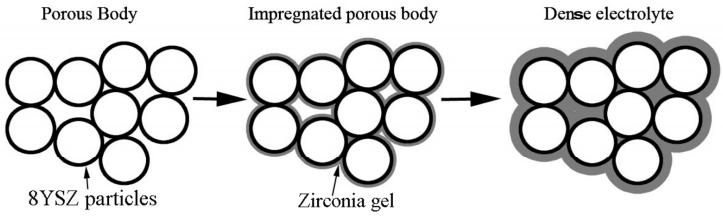

Fig. 1. Schematic steps of preparation of dense electrolyte by net shape forming

2. EXPERIMENTAL PROCEDURE

8YSZ powder (8Y- TZP, TOSOH, Tokyo, Japan,) and polyvinyl alcohol (Aldrich) were used as starting materials. To prepare a porous body skeleton, 8YSZ powder was mixed with 2 wt.% polyvinyl alcohol (based on powder weight) solution in water. The resulting mixture was then dried in an oven. Dried powders were then formed into cylindrical pellets of diameter of 25 mm and thickness 2 - 3 mm by combination of uniaxial compression (P = 40 MPa) followed by isostatic pressing (P = 200 MPa). The cylindrical pellets were the heated to 800 °C by heating rate of 1 K/min and were kept at that temperature for 2 hours to remove PVA whilst retaining near net shape.

The prepared porous pellets were immersed in solution of zirconium (IV) aceylacetonate (Aldrich, 98%) in water and were impregnated under vacuum. Two different average compositions with 7.6 mol% yttria ($7.6YSZ_{net}$) and 6.9 mol% yttria ($6.9YSZ_{net}$) were prepared. The impregnated samples were annealed at 600 °C for 1h (with heating rate of 1 K /min). Repeated impregnation- annealing was performed to increase the zirconia content of porous pellets. After annealing, the pellets were sintered at, 1350°C for 10 h under air. It should be noted that up to seven cycles of impregnation-annealing was required to achieve samples with 6.9 mol% yttria content. The density of the sintered samples was measured by the Archimedes procedure.

The Polished and chemically etched samples (using hot sulfuric acid) were investigated by means of scanning electron microscopy (SEM, JEOL, JSM-56000) to reveal the microstructure. The EDX Inca Energy System (equipped on SEM) was used to identify local composition distribution of the samples. The average grain size was measured by the linear intercept length method [13].

Phase analysis was carried out on sintered samples by X-ray powder diffraction (XRD) using a STOE Stadi P transmission diffractometer (Cu $K\alpha 1$ = 1.5406 Å). At first, XRD measurements were performed over 2θ range of 26° -90° with a step width of 0.05° and 30 seconds of exposure time per position. Because of structural similarity of cubic and tetragonal phases, XRD diffraction peaks have some common strong peaks [14]. To confirm the presence of both cubic and tetragonal phases and calculate the amount of each phase, XRD measurements were also performed in a narrower 2è range from 70° to 76° with a step size of 0.05° and 50 seconds of exposure time per step. The program GSAS was implemented for Reitveld refinement of XRD data [15]. The refinement was performed by various combinations of space groups including cubic (FM3M), tetragonal (P42/NMC) and monoclinic (P121/C1) after subtraction of background.

Ionic conductivities were measured using Hewlett Packard 4192A impedance analyzer over the frequency range 5Hz-13MHz at temperatures 300 – 900 °C with Pt paste electrodes in air. The electrical conductivity was recorded during cooling at 50° C intervals. The applied a.c voltage in all impedance measurements was 0.1V.

Hardness and toughness of the sintered samples were measured by Vickers micro indentation method on polished surfaces (dawn to 1 μm diamond paste) by hardness tester (Matsuzawa, model MHT2, Yamamoto, Japan) under load of 98 N. The formula of Anstis (16) was used to calculate fracture toughness, using an elastic modulus (E) of 200 GPa [17].

Biaxial flexural strength of disc type specimens was measured by ring on ring test

method according to the ISO 6474 standard test method [18]. A universal testing machine ZWICK (Model 1496-2D, Germany) with cross head speed of 0.1 mm/min, was used to perform the test on specimens with diameter of 20 mm and thickness of at least 2 mm. Measurement of hardness, toughness and strength was performed on at least 5 different samples and data are reported as an average.

3. RESULTS AND DISCUSSION

3. 1. Sample Characteristic and Microstructure

Table 1 presents the nomenclature, composition and density of the samples. To prepare $6.9YSZ_{net}$ sample, seven cycles of impregnation/annealing was performed. All samples show good density (higher than 96% of theoretical density) after sintering which is desirable for electrical and mechanical properties investigations. The theoretical density of pure 8YSZ and 3YSZ are 5.9 and 6.01 g/cm^3 respectively. The results of XRD analysis of the samples over 2 θ range of 26 to 90° along with the residual curve after refinement is presented in Fig. 2. The refinement converges with reasonable R values. The resulting unit cell parameters and amount of each phase are presented in Table 2. The calculated lattice parameters are in good agreement with previously reported data [14].

According to JCPDS card 42-1164 and 27-0997, diffraction profiles of both cubic and tetragonal zirconia are present in $6.9YSZ_{net}$ sample. As the XRD profiles of tetragonal and cubic phase of zirconia overlap, usually the

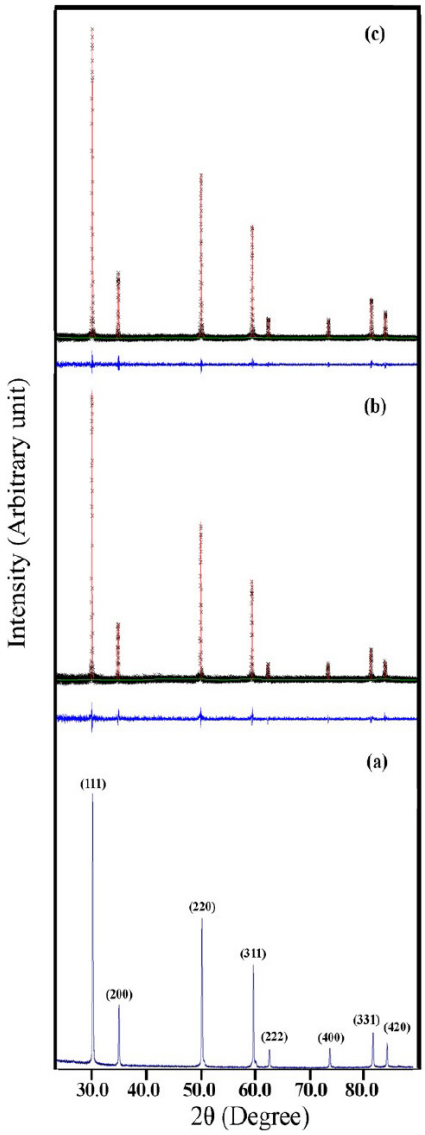

Fig. 2. XRD pattern of pure 8YSZ (a), $7.6YSZ_{net}$ (b) and $6.9YSZ_{net}$ (c) samples over 2 θ form 26 to 90 °.

Table 1. Nomenclature, composition, density and grain size of samples

Sample	Composition (Y2O3 mol%)	Density (gcm^{-3})	Grian size (μm)	
			Cubic zirconia	Tetragonal zirconia
8YSZ(TZ-8Y, Tosoh)	8	5.6	5	-
$7.6YSZ_{net}$	7.6	5.4	5	-
$6.9YSZ_{net}$	6.9	5.6	4	0.3

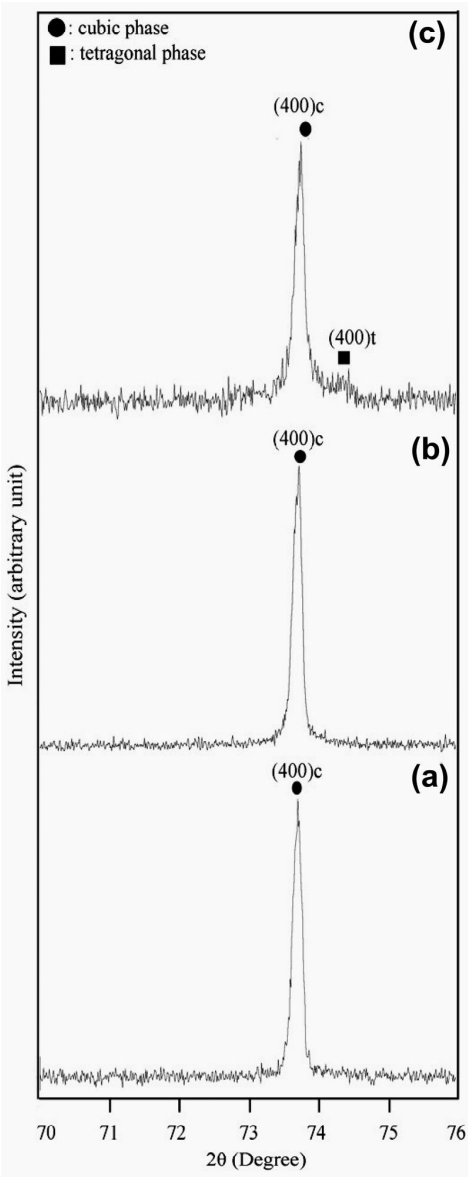

Fig. 3. XRD pattern of pure 8YSZ (a), 7.6YSZ$_{net}$ (b) and 6.9YSZ$_{net}$ (c) samples over 2 θ form 70 to 76 °.

(400)t and (004)t peaks of tetragonal and (400)c of cubic phase peak, are used to distinguish the presence and calculation the amount of these two phases. These peaks are appeared over 2 θ range of 70 80 ° and Fig. 3 compares the recorded XRD pattern of pure 8YSZ, 7.6YSZ$_{net}$ and 7.6YSZ$_{net}$ samples over this 2 θ range. It is obvious that both pure 8YSZ and 7.6YSZ$_{net}$ samples do not show the presence of tetragonal phase peaks while XRD peaks of both tetragonal and cubic phase are present in the 6.9YSZ$_{net}$ sample so it can be said that tetragonal phase amount in 7.6YSZ$_{net}$ samples is below the detection limit of XRD analysis.

The SEM image of pure 8YSZ, 7.6YSZ$_{net}$ and 6.9YSZ$_{net}$ samples are presented in Fig 4. The average grain sizes of samples are shown in Table 1. Grain size of sintered ceramics depends on many factors including sintering conditions, impurity and phase content. It has been reported that the grain size of sintered pure 8YSZ varies between 5-20 μm [1] while the grain size of sintered 3YSZ is around 0.3- 0.5 μm [8]. It should be noted that under excessive grain growth, tetragonal phase changes to monoclinic phase spontaneously which degrade both mechanical and electrical properties of 3YSZ. The reported grain sizes in Table 1 are consistent with reported data. However the lower grain size of cubic phase in 6.9YSZ samples may be due to presence of tetragonal second phase which inhibit grain growth of cubic phase.

The microstructure of pure 8YSZ and 7.6YSZ$_{net}$ samples consist of large grain which is the characteristic of cubic phase structure while the microstructure of 6.9YSZ$_{net}$ sample shows bimodal grain size distribution that is composed of fine tetragonal and larger cubic grains. Fig. 4d and 4e show the microstructure of porous body and impregnated samples respectively. In addition Fig.4 (f) shows the cracks which some times appear in the impregnated samples after multi impregnation and annealing for much higher impregnation cycles. These cracks lower the mechanical strength of prepared samples.

3. 2. Electrical Properties

The contribution of bulk and grain boundary resistivity to the total ceramic resistance for each sample was estimated using impedance spectroscopy. All of the plots show decrease of conductivity with decreasing temperature which is due to the lower vacancy mobility at lower temperatures. In addition, a change in slope of the Arrhenius plot occurs at low temperatures (~ T= 550 °C). The change in slope of Arrhenius plot which is the change in activation energy of conductivity has been attributed to the association-dissociation of defect clusters [2]. At low temperature some defects makes double or

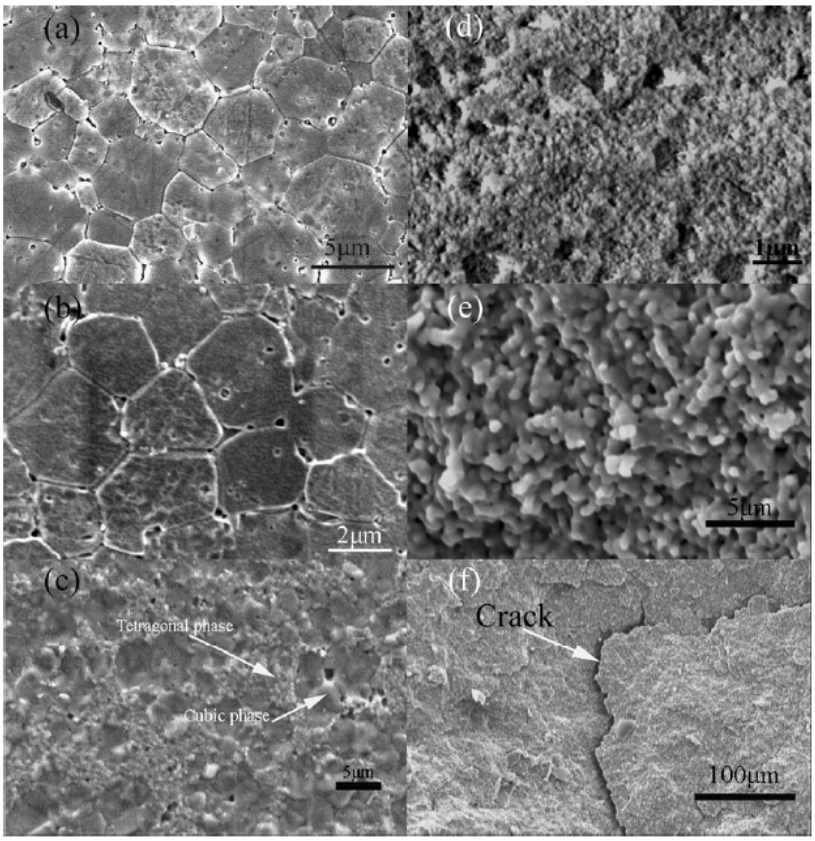

Fig. 4. SEM micrograph of pure 8YSZ (a), 7.6YSZ$_{net}$ (b), 6.9YSZ$_{net}$ (c), porous body after binder removal at 600 °C (d), impregnated body after annealing at 800°C (e) and fracture surface of some impregnated bodies (f)

Table 2. Phase content, lattice parameters and R values of different sample obtained from reitveld refinement

Specimen	Phase content (wt.%)		Lattice parameters (A°)			R values		
	Cubic	tetragonal	Cubic	Tetragonal		R_{wp}	R_p	χ^2
			a	a	c			
8YSZ	100	-	5.139(01)	-	-	14	11	1.6
7.6YSZ$_{net}$	100	-	5.139(01)	-	-	13	12	1.5
6.9YSZ$_{net}$	83	17	5.137 (01)	3.62(02)	5.14(02)	15	12	1.7

triple pairs which has a lower mobility with respect to free defects.

It is well documented that the impedance response of the ceramic materials relates geometry and nature of response (e.g. bulk, grain boundary or electrode) to the associated capacitance [19]. For a bulk type response one would expect capacitance of the order of pF and

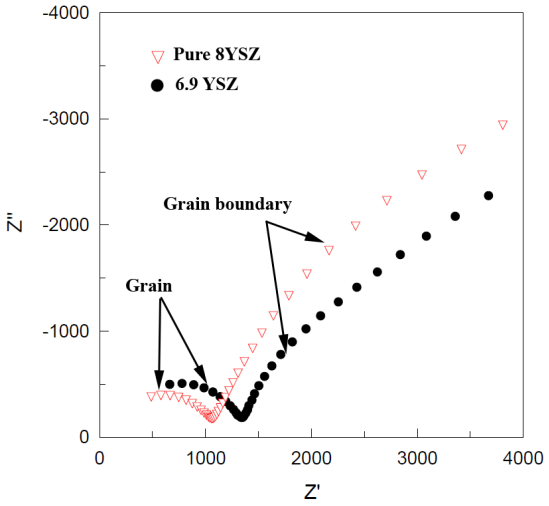

Fig. 5. Temperature dependence of total conductivity of various samples

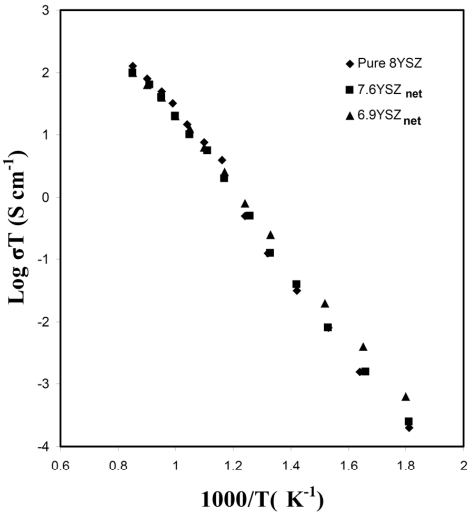

Fig. 6. Temperature dependence of bulk conductivity of samples at low temperatures (T< 550 °C)

for grain boundary type response one would expect a response of nF cm. In this approach the constant dielectric of superionic conductor materials is relatively independent of composition and varies less than an order of magnitude [19]. In the low temperature range (280 – 450 °C) two semi circles are observed in the impedance plot. The calculated capacitance values have been presented in Table 3. The high frequency arc is the bulk component and low frequency arc correspond to grain boundary component. Because of depression of the arcs in some cases, the use of simple capacitor is not sufficient to model the electrical response of the materials so more complex equivalent circuit with frequency-dependent elements such as constant phase elements is used to fit results. The impedance spectra can be modelled with a series of three electrical circuits, having resistance and constant phase element coupled in parallel. Fig. 5 compares typical impedance spectra of pure 8YSZ and 6.9YSZ at 233 °C, in which bulk and grain boundary arcs are clearly observed.

The Arrhenius plot of total conductivity is shown in Fig 6. The corresponding curve for pure 8YSZ prepared under the same condition has been presented for the sake of comparison. The electrical behaviour of pure 8YSZ and 7.6YSZ$_{net}$ samples are the same which is acceptable according to their similar phase content and microstructure. The calculated conductivity of pure 8YSZ in this study was 0.1 S/cm at 900 °C which is in good agreement with other reported data [3,9]. The calculated activation energies of pure 8YSZ and 7.6YSZ$_{net}$ at both high and low temperatures are also similar (Table 3). The

Table 3. Activation energy and conductivity of various samples

Specimen	Activation energy (eV)		Calculated capacitance values (F/cm) *	
	High-temperature section (T< 550°C, $E_a \pm 0.04$)	Low-temperature section (T> 550, Ea ± 0.04)	Bulk	Grain boundary
8YSZ	0.94	1.08	5.6×10^{-12}	6.7×10^{-9}
7.6YSZ$_{net}$	0.98	1.10	5.04×10^{-12}	7.8×10^{-9}
6.9YSZ$_{net}$	0.96	1.04	5.8×10^{-12}	8.2×10^{-9}
6.9YSZ$_{net}$- after annealing	0.96	1.06	6.4×10^{-12}	3.19×10^{-9}

* Capacitance values are fairly constant

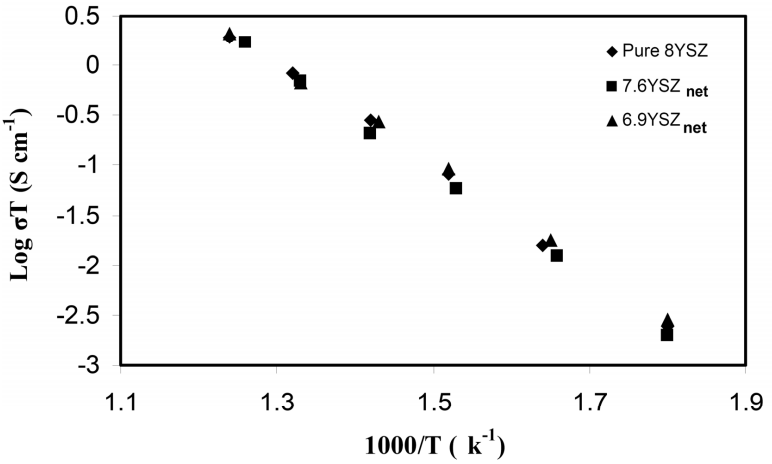

Fig. 7. Temperature dependence of bulk conductivity of samples at low temperatures (T< 550 °C)

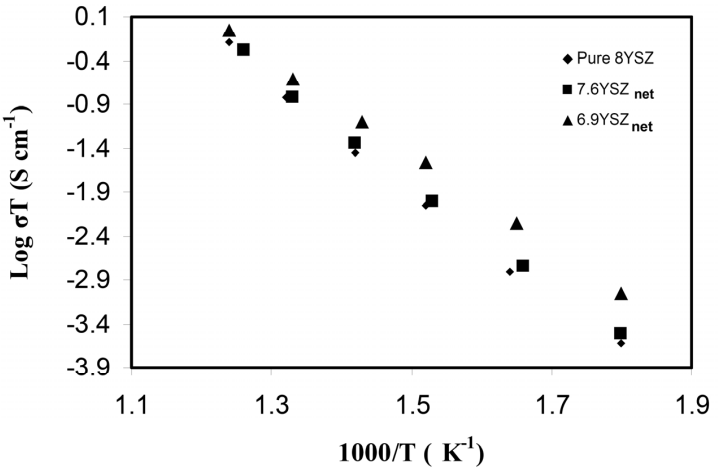

Fig. 8. Temperature dependence of total conductivity of 6.9YSZ$_{net}$ sample before and after annealing

calculated activation energy for pure 8YSZ is comparable to other researches [1,7,9]. However, the sample 6.9YSZ$_{net}$ shows slightly higher conductivity at low temperatures which can be related to its higher tetragonal phase content. It has been reported that the bulk conductivity of tetragonal phase is higher than the conductivity of 8YSZ [1]. The measured activation energies of 6.9YSZ$_{net}$ sample are also presented in Table 3.

To investigate the effect of the tetragonal second phase on electrical properties of the 8YSZ, matrix the Arrhenius plot of bulk and grain boundary conductivity of the samples at low temperature range are presented in Figs.7 and 8 respectively. As can be seen, all the samples have roughly the same bulk conductivity while the sample 6.9YSZ with high tetragonal phase content, has higher grain boundary conductivity. The higher conductivity of 6.9YSZ at low temperatures can be related to at least two reasons: 1- The higher amount of tetragonal phase in 6.9YSZ sample which has a higher bulk electrical conductivity with respect to cubic phase at low temperatures, 2- The higher grain boundary conductivity of 6.9YSZ sample (Fig. 8) or the lower grain boundary contribution to total conductivity which is also addressed by impedance spectra (Fig. 4).

In general, grain boundaries are the major reason of low electrical conductivity of solid electrolytes, especially at low temperatures. Addition of second phases can lower grain boundary contribution to total conductivity of solid electrolytes, an effect which is called

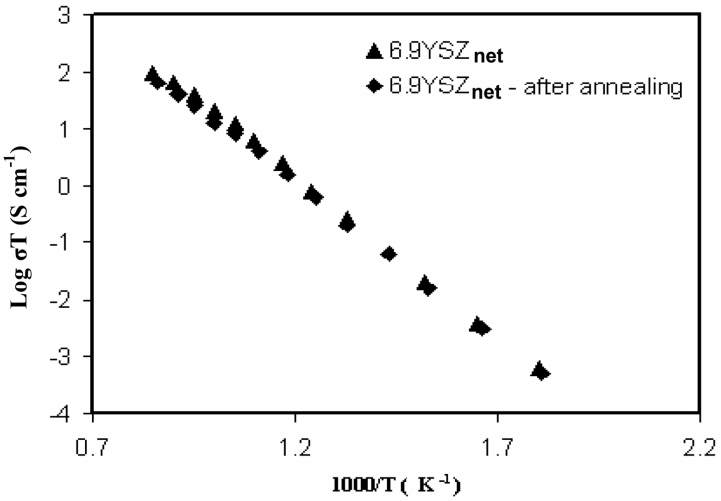

Fig. 9. Temperature dependence of total conductivity of 6.9YSZ$_{net}$ sample before and after annealing

"composite effect" [20]. Impedance analysis reported in this study showed that composite samples had lower grain boundary contribution to total conductivity which may be due to the composite effect.

The values of the activation energies of the bulk and grain boundary conductivities are summarised in Table 3. Fairly lower activation energy of 6.9 samples can be due to the lower activation energy of tetragonal phase with respect to cubic phase [1].

Fig. 9 compares the electrical conductivity of 6.9YSZ sample before and after annealing. Annealing at 1000°C for 170 h has decreased the conductivity at 900 °C by 33%.

3. 3. Mechanical Properties

Table 5 compares the mechanical properties of the samples. It is obvious that multi impregnation which has increased the tetragonal phase content of 6.9YSZ sample, has improved mechanical properties. Increasing the amount of tetragonal phase increases hardness, fracture strength and fracture toughness of 8ysz matrix phase. It is common knowledge that tetragonal zirconia with 2-3 mol% yttria content can improve mechanical properties of zirconia containing ceramics by the phenomena called transformation toughening [8]. The tetragonal to monoclinic phase transformation at crack tips which can hinder crack growth [8].

In addition, toughness of pure 8YSZ and 3YSZ raw materials prepared under the same condition are 1.7 MPa.m$^{1/2}$ and 5.8 MPa.m$^{1/2}$ respectively. The reported fracture toughness of 8YSZ ceramics vary over a range of 0.9-3 MPa.m$^{1/2}$, depending on test method and form of the material (pressed bar or thin foil) [7]. Measured toughness values of pure 3YSZ are different, being primarily dependent on parameters like starting powder, sintering parameter, microstructure variables and testing technique [21].It is well established that grain size strongly

Table 4. Mechanical properties of 8YSZ and 6.9YSZ samples

Material	Hardness* (GPa)	Fracture Toughness* K_{IC}(MPa m$^{1/2}$)	Mean fracture* strength (MPa)
8YSZ	12.7	1.7	156
6.9YSZ$_{net}$	12.8	2.54	254

* Values are reported as an average of 5 measurements

influences the toughness of 3YSZ ceramic specimens [21]. The reported fracture toughness of 3YSZ samples (TZ-3Y, Tosoh, Tokyo, Japan) with an average grain size of ~ 0.5 μm is about 6 $MPa.m^{1/2}$ [21].

The reported fracture strength of pure 3YSZ and 8YSZ are also varies between 800-1700 MPa and 160-350 MPa respectively [21,7]. It is important to remember that fracture strength of brittle materials is not a characteristic material property, but depends on the size of flaws and their distribution, which in turn depends on the fabrication process, specimen size and testing methods [22]. According to measured fracture toughness and fracture strength in the present work, sample $6.9YSZ_{net}$ with higher tetragonal phase content show improved mechanical properties with respect to pure 8YSZ.

4. CONCLUSION

It was shown that zirconia based solid electrolytes with intermingled tetragonal/cubic structure, could be prepared using net shape forming. Only after multi impregnation cycles did the tetragonal phase appear. Increasing tetragonal phase content of solid electrolytes increased both fracture toughness and strength noticeably while the electrical conductivity at high temperatures was not highly affected. In addition, the conductivity of samples at low temperatures increased with increasing the amount of tetragonal phase. Activation energies of conductivity at both low and high temperatures were lowered by the presence of tetragonal phase.

REFERENCES

1. Badwal, S. P. S., Zirconia Based Electrolytes: Stability, Microstructure, and Ionic Conductivity, Solid State Ionics, 1992, 52, 23.
2. Feighery, A.J. and Irvine, J.T.S., Effect of Alumina Additions upon Electrical Properties of 8 mol% Yttria-Stabilised Zirconia, Solid State Ionics, 1999, 121, 209.
3. Riegel, J., Neumann, H. and Wiedenmann, H .M., Exhaust gas sensors for automotive emission control, Solid State Ionics, 20002, 152–153, 783.
4. Mori, M., Abe, T., Itoh, H., Yamamoto, O., Takeda, Y. and Kawahara, T., Cubic- Stabilized Zirconia and Alumina Composites as Electrolytes in Planar Type Solid Oxide Fuel-Cells, Solid State Ionics, 1994, 74, 157.
5. Liu, X.Q. and Chen, X. M., Toughening of 8Y-FSZ Ceramics by Neodymium Titanate Secondary Phase, J. Am. Ceram. Soc., 2005, 88, 456.
6. Liu, X.Q. and Chen, X.M., Microstructures and Mechanical Properties of 8Y-FSZ Ceramics with BaTiO3Additive, Ceram. Int., 2004, 30, 2269.
7. Minh, N. Q., Ceramic Fuel Cells, J. Am. Ceram. Soc., 1993, 76, 563.
8. Hannink, R. H. J., Kelly, P. M. and Muddle, B. C., Transformation Toughening in Zirconia-Containing Ceramics, J. Am. Ceram. Soc., 2000, 83, 461.
9. Meyer, D., Eisele, U., Sateta, R. and Rodel, J., Codoping of Zirconia with Yttria and Scandia, Scr. Mater., 2008, 58, 215.
10. Jasinski, P., Suzuki, T., Petrovsky, V. and Anderson, H. U., Electrical Properties of YSZ Films Prepared by Net Shape Technology, Solid-State Lett., 2005, 8, A219.
11. Jiang, S. P. and Wang, W., Novel Structured Mixed Ionic and Electronic Conducting Cathodes of Solid Oxide Fuel Cells, Solid State Ionics, 2005, 176, 1351.
12. Jiang, S. P., Zhang, S., Zhen, Y. D and Wang, Fabrication and performance of impregnated Ni anodes of solid oxide fuel cells, W., J. Am. Ceram. Soc., 2005, 88, 1779.
13. Mendelson M. I., Average Grain Size in Polycrystalline Ceramics, J. Am. Ceram. Soc., 1969, 52, 443.
14. Paterson, A. and Stevens, R., Phase Analysis of Sintered Yttria-Zirconia Ceramics by X-ray Diffraction, J. Mater. Res., 1986, 1, 295.
15. McCusker, L. B., Von Dreele, R. B., Cox, D. E., Loued, D. and Scardi, P., Reitveld Refinement Guidelines, J. Appl. Crystallogr., 1999, 32, 36.
16. Anstis, G. R., Chantiku, P., Lawn, B. R. and Marshall, D. B., A Critical Evaluation of Indentation Techniques for Measuring Fracture Toughness: I, Direct Crack Measurements, J. Am.Ceram. Soc., 1981, 64, 533.

17. Adams, J. W., Ruh, R. and Mazdiyasni, K. S., Young s Modulus, Flexural Strength, and Fracture of Yttria-Stabilized Zirconia Versus Temperature, J. Am. Ceram. Soc., 1997, 80, 903.
18. Standard ISO 6474, Implants for Surgery – Ceramic Materials Based on High Purity Alumina, 1994.
19. Irvine, J. T. S., Sinclair, D. C. and West, A. R., Electroceramics: Characterization by Impedance Spectroscopy, Adv. Mater., 1990, 2,132.
20. Filal, M., Petot, C., Mokchah, M., Chateau, C. and Carpentier, J. L., Ionic Conductivity of Yttrium-Doped Zirconia and The Composite Effect, Solid state Ionics, 1995, 80, 27.
21. Basu B., Toughening of Yttria-Stabilised Tetragonal Zirconia Ceramics, Int. Mater. Rev., 2005, 50, 239.
22. Atkinson, A. and Selcuk, A., Mechanical Behaviour of Ceramic Oxygen Ion Conducting Membranes, Solid State Ionics, 2000, 134, 59.